REPORT DOCUMENTATION PAGE

Form Approved OMB No. 0704-0188

1. REPORT DATE *(DD-MM-YYYY)*	2. REPORT TYPE	3. DATES COVERED *(From - To)*
11/8/2006	Final Technical	Jan 1 2004-Dec 31 2005

Development of Advanced Hall Plume Models

5a. CONTRACT NUMBER

5b. GRANT NUMBER
FA9550-04-1-0033

5c. PROGRAM ELEMENT NUMBER

6. AUTHOR(S)
Jaume Peraire Manuel Martinez-Sanchez

5d. PROJECT NUMBER

5e. TASK NUMBER

5f. WORK UNIT NUMBER

7. PERFORMING ORGANIZATION NAME(S) AND ADDRESS(ES)

MIT, Department of
Aeronautics and Astronautics

8. PERFORMING ORGANIZATION REPORT NUMBER

9. SPONSORING / MONITORING AGENCY NAME(S) AND ADDRESS(ES)

Joseph G. Banuls
(703) 696-9545
AF Office of Scientific Research
875 N. Randolf St. Suite 325
Room 3112
Arlington, VA 22203

10. SPONSOR/MONITOR'S ACRONYM(S)
AFOSR/PKC

11. SPONSOR/MONITOR'S REPORT NUMBER(S)
AFRL-SR-AR-TR-06-0403

12. DISTRIBUTION / AVAILABILITY STATEMENT

Approved for public release,
distribution unlimited

13. SUPPLEMENTARY NOTES

14. ABSTRACT

The purpose of this work was twofold: (a) To develop numerical or analytical methods capable of dealing with the combination of three-dimensionality and strong anisotropy that occurs in the plume region near the exit of a Hall thruster, and (b) To explore the use of fluid-based models in plume computations, so as to overcome the granularity associated with normal particle-based approaches. In area (a) we have carefully formulated the 3D near-plume problem using a combination of heavy particle tracking and magnetized electron fluid equations, and have to a large extent clarified the structure of the solutions, such that numerical implementation should be greatly facilitated. In area (b) we have concentrated on an examination of the far-field of the plume, where the geomagnetic field takes over the dynamics. Again, only a formulation and a suggested method for numerical implementation were completed. Two graduate Theses are still in progress in these two areas, and we expect to issue a supplementary report when they are finalized.

15. SUBJECT TERMS

16. SECURITY CLASSIFICATION OF:			17. LIMITATION OF ABSTRACT	18. NUMBER OF PAGES	19a. NAME OF RESPONSIBLE PERSON
a. REPORT	b. ABSTRACT	c. THIS PAGE			19b. TELEPHONE NUMBER *(include area code)*
U	U	U	UU	25	

Development of Advanced Hall Plume Models

Final Technical Report on AFOSR Grant FA9550-04-1-0033 (MIT 6895852)

By Jaume Peraire and Manuel Martinez-Sanchez

MIT, Department of Aeronautics and Astronautics

August 11, 2006

Abstract

The purpose of this work was twofold: (a) To develop numerical or analytical methods capable of dealing with the combination of three-dimensionality and strong anisotropy that occurs in the plume region near the exit of a Hall thruster, and (b) To explore the use of fluid-based models in plume computations, so as to overcome the granularity associated with normal particle-based approaches. In area (a) we have carefully formulated the 3D near-plume problem using a combination of heavy particle tracking and magnetized electron fluid equations, and have to a large extent clarified the structure of the solutions, such that numerical implementation should be greatly facilitated. In area (b) we have concentrated on an examination of the far-field of the plume, where the geomagnetic field takes over the dynamics. Again, only a formulation and a suggested method for numerical implementation were completed. Two graduate Theses are still in progress in these two areas, and we expect to issue a supplementary report when they are finalized.

Content

1 Near-exit plume model

1.1 Introduction

A multiplicity of plume codes based on hybrid simulation has been developed by many researchers [1,2,3,4] these codes mature and comparisons are attempted to lab or space plume data, it becomes evident that one of the essential ingredients is the distributions of density, velocity and temperature of the ions at the initial plane, which is either the thruster exit plane, or a plane chosen some short distance downstream from the exit. Our work intends to improve present models for initial plane distributions in Hall thrusters by solving accurately the near-exit zone.

The near-exit plume is characterized by different aspects that are not covered in the usual plume models:

- Strong magnetic field.
- Ionization.
- 3D effects in the electron population induced by the hollow cathode.

Such effects can be taken into account by a hybrid model. Heavy particles, ions and neutrals, are modeled using Particle-In-Cell (PIC) methods, whereas electrons are considered as a continuum. The main difference with respect to previous hybrid plume model is in the electron treatment, which includes the 3D anisotropy induced by the magnetic field.

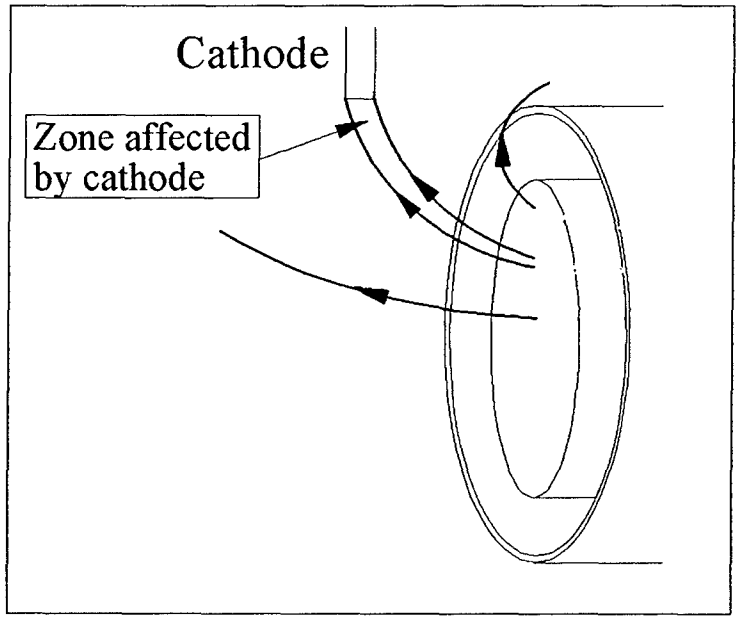

Figure 1.1 Near-exit plume diagram. The cathode induces a highly anisotropic profile. Due to the fast diffusion along the magnetic field lines, its effect extends far.

Figure 1.1 presents the typical geometry in the near-exit plume. Even though the geometry of the acceleration channel and the magnetic field is axi-symmetric, the cathode breaks the symmetry. The diffusion along the magnetic lines is much larger than the perpendicular diffusion. Thus, the cathode imposes the electron temperature and the electric potential on the magnetic lines that touch it. The effect of the cathode extends really far due to the fast diffusion along the magnetic lines. This effect and its range is difficult to model because the transport across the magnetic lines has two components very different in nature and value: the diamagnetic transport, perpendicular to the driving potential gradient, modified by the pressure gradient, and the collisional perpendicular transport. The diamagnetic transport is closely related to the $E \times B$ drift and it is a consequence of the Larmor motion. The collisional perpendicular transport, much smaller in size, has to do with perturbations on the Larmor motion, such as collisions or turbulence. Note that in the axi-symmetric models, the diamagnetic transport lays in the azimuthal direction, balancing out. However, in a 3D case, such as this one, this transport has to be taken into account because it is the most important contribution in the direction perpendicular to the magnetic field.

In what follows we discuss the electron fluid equations and the special mathematical difficulties that appear as a consequence of the combination of strong magnetization and three-dimensionality.

1.2 Electron equations

Electrons are modeled as a continuum. The equations to be solved are charge, momentum and energy conservation.

Since the Larmor radius is really small compared to the typical length in the problem, a simple diffusive model is proposed for all these equations. Such an approximation is acceptable for the motion perpendicular to the magnetic field lines, but it is not as correct along the lines. However, the proposed model is expected to yield results that contain most of the physics.

In the next subsections, the different equations are described and explained briefly.

1.2.1 Charge conservation

Assuming quasineutrality:

$$\nabla \cdot \mathbf{j}_i + \nabla \cdot \mathbf{j}_e = 0 \tag{1.1}$$

$\mathbf{j}_i$ is the ion current density, and it is obtained in the PIC submodel. $\mathbf{j}_e = -en_e\mathbf{v}_e$ is the electron current density. It is one of the unknowns that must be obtained from the electron equations.

Momentum conservation

In the diffusive limit:

$$0 = -\frac{1}{m_e}\nabla(n_e T_e) + \frac{e n_e}{m_e}\nabla\phi + \frac{1}{e}\omega_e \mathbf{j}_e \times \hat{\mathbf{b}} + \frac{1}{e}\nu_e \mathbf{j}_e \tag{1.2}$$

where ϕ is the electrostatic potential, T_e the electron temperature, $\omega_e = eB/m_e$ is the gyrofrequency, $\hat{\mathbf{b}} = \mathbf{B}/B$ is the unit vector in the same direction as the magnetic field and ν_e is a frequency that measures the collisionality and turbulence.

$\mathbf{j}_e$ can be solved from this equation:

$$\mathbf{j}_e = j_{eb}\hat{\mathbf{b}} + \mathbf{j}_{eH} + \mathbf{j}_{e\perp} \tag{1.3}$$

where

$$j_{eb} = -\sigma_b \hat{\mathbf{b}} \cdot \left[\nabla\phi^* + \frac{1}{e}\nabla T_e(\ln n_e - 1)\right] \tag{1.4}$$

$$\mathbf{j}_{eH} = -\sigma_H \hat{\mathbf{b}} \times \left[\nabla\phi^* + \frac{1}{e}\nabla T_e(\ln n_e - 1)\right] \tag{1.5}$$

$$\mathbf{j}_{e\perp} = -\sigma_\perp \left[\nabla_\perp\phi^* + \frac{1}{e}\nabla_\perp T_e(\ln n_e - 1)\right] \tag{1.6}$$

j_{eb} is the current along the magnetic field line. $\mathbf{j}_{eH}$ is the diamagnetic component of the current. It contains the electron current due to the $E \times B$ drift, plus the curvature and ∇B drifts. $\mathbf{j}_{e\perp}$ is the collisional perpendicular current. It accounts for collisions and turbulence.

It is important to point out that in axi-symmetric cases, $\mathbf{j}_{eH}$ is aimed in the azimuthal direction, therefore cancelling exactly. Thus, it is not usually included in 2D models.

In these equations, the *thermalized potential*, ϕ^*, is used. It is defined as:

$$\phi^* = \phi - \frac{T_e}{e}\ln n_e \tag{1.7}$$

$\nabla_\perp = \nabla - \hat{\mathbf{b}}\hat{\mathbf{b}} \cdot \nabla$ is the gradient in the perpendicular direction to the magnetic field.

The conductivity for the plasma is different in the different spatial directions. In equations1.4, 1.5 and1.6, these conductivities are called σ_b, σ_H and $\sigma_\perp$:

$$\sigma_b = \frac{e^2 n_e}{m_e \nu_e} \tag{1.8}$$

$$\sigma_H = \frac{e^2 n_e}{m_e} \frac{\omega_e}{\omega_e^2 + \nu_e^2} \approx \frac{e n_e}{B} \quad (\nu_e << \omega_e) \tag{1.9}$$

$$\sigma_\perp = \frac{e^2 n_e}{m_e} \frac{\nu_e}{\omega_e^2 + \nu_e^2} \tag{1.10}$$

Considering that $\nu_e << \omega_e$ near the exit:

$\sigma_b >> \sigma_H >> \sigma_\perp$

The ratio between these different conductivities is the hall parameter, $\beta_H = \omega_e / \nu_e$. For example, $\sigma_b / \sigma_H \sim \beta_H$, or $\sigma_H / \sigma_\perp \sim \beta_H$. This means that the plasma tends to homogenize much faster along the magnetic lines, where σ_b is the conductivity. Then, along the magnetic lines:

$$\hat{\mathbf{b}} \cdot \nabla \phi^* - \frac{1}{e} \hat{\mathbf{b}} \cdot \nabla T_e (\ln n_e - 1) = 0 \tag{1.11}$$

Actually, from the energy equation, we will obtain that $\hat{\mathbf{b}} \cdot \nabla T_e = 0$, which means that 1.11 is:

$$\hat{\mathbf{b}} \cdot \nabla \phi^* = 0 \tag{1.12}$$

Even though $\hat{\mathbf{b}} \cdot \nabla \phi^* = 0$ and $\hat{\mathbf{b}} \cdot \nabla T_e = 0$, j_{eb} is non-zero.

Plugging equation 1.3 into 1.1:

$$\nabla \times (\hat{\mathbf{b}} \sigma_H) \cdot \nabla \phi^* + \nabla \cdot (\sigma_\perp \nabla_\perp \phi^*) - \nabla \times (\hat{\mathbf{b}} \gamma_H) \cdot \nabla (T_e / e) - \nabla \cdot (\gamma_\perp \nabla_\perp (T_e / e)) = \\ = \nabla \cdot \mathbf{j}_i + \nabla \cdot (\hat{\mathbf{b}} j_{eb}) \tag{1.13}$$

$\gamma_j = \sigma_j (\ln n_e - 1)$, where $j = H, \perp$.

It is important to note that in this equation there are terms of very different order of magnitude. The terms that contain σ_H and γ_H are larger by a factor ω_e / ν_e, provided the other factors in them are comparable to those in other terms.

1.2.3 Energy conservation

The energy conservation is given by:

$$\frac{\partial}{\partial t}\left(\frac{3}{2}n_e T_e\right)+\nabla\cdot\left(-\mathbf{j}_e\frac{5}{2}\frac{T_e}{e}+\mathbf{q}_e\right)=-\mathbf{j}_e\cdot\nabla\phi-n_e\nu_i\alpha E_i \tag{1.14}$$

where $\mathbf{q}_e$ is the electron heat conduction flux, and $n_e\nu_i\alpha E_i$ are the ionization losses.

The heat conduction can be obtained using a diffusive approximation, similar to the one used to obtain the electron current density (equation 1.3):

$$\mathbf{q}_e = q_{eb}\hat{\mathbf{b}}+\mathbf{q}_{eH}+\mathbf{q}_{e\perp} \tag{1.15}$$

where

$$q_{eb} = -\kappa_b\hat{\mathbf{b}}\cdot\nabla T_e \tag{1.16}$$

$$\mathbf{q}_{eH} = -\kappa_H\hat{\mathbf{b}}\times\nabla T_e \tag{1.17}$$

$$\mathbf{q}_{e\perp} = -\kappa_\perp\nabla_\perp T_e \tag{1.18}$$

Thermal conductivity is highly anisotropic. The values of the different coefficients are:

$$\kappa_b = \frac{5}{2}\frac{n_e T_e}{m_e\nu_e} \tag{1.19}$$

$$\kappa_H = \frac{5}{2}\frac{n_e T_e}{m_e}\frac{\omega_e}{\omega_e^2+\nu_e^2} \tag{1.20}$$

$$\kappa_\perp = \frac{5}{2}\frac{n_e T_e}{m_e}\frac{\nu_e}{\omega_e^2+\nu_e^2} \tag{1.21}$$

For $\omega_e >> \nu_e$, the coefficients have really different orders of magnitude:

$\kappa_b >> \kappa_H >> \kappa_\perp$

As it happened with the electrical conductivities, the ratio between the different thermal conductivities is the Hall parameter.

Thermal diffusion is high in the direction of the magnetic field. That means that, as a first approximation, the temperature is constant along the lines:

$$\hat{\mathbf{b}}\cdot\nabla T_e = 0 \tag{1.22}$$

Even though $\hat{\mathbf{b}}\cdot\nabla T_e$ is almost zero, q_{eb} is not zero. That means that equation 1.14 can be written as:

$$\begin{aligned}\frac{3}{2}en_e\frac{\partial}{\partial t}\left(\frac{T_e}{e}\right)+\nabla\cdot\left[\hat{\mathbf{b}}q_{eb}-\hat{\mathbf{b}}\left(\left(\frac{5}{2}-\ln n_e\right)\frac{T_e}{e}-\phi^*\right)j_{eb}\right]+\\ +\nabla\times(\hat{\mathbf{b}}\Sigma_H)\cdot\nabla\phi^*+\nabla\cdot(\Sigma_\perp\nabla_\perp\phi^*)-\\ -\nabla\times(\hat{\mathbf{b}}\Gamma_H)\cdot\nabla\left(\frac{T_e}{e}\right)-\nabla\cdot\left(\Gamma_\perp\nabla_\perp\left(\frac{T_e}{e}\right)\right)=\\ =-\left[\left(\frac{3}{2}-\ln n_e\right)\frac{T_e}{e}-\phi^*\right]\frac{\partial}{\partial t}(en_e)+en_e\nu_i\left(-\alpha\frac{E_i}{e}-\frac{T_e}{e}\ln n_e-\phi^*\right)\end{aligned} \tag{1.23}$$

The first term in the LHS is just the time variation term for temperature. The second term is the energy transport along the magnetic field lines. We would eliminate this term by integrating along the magnetic lines. Note that the energy transport includes the potential energy, $-en_e\phi$. This potential energy transport can be obtained from the Joule heating term, as we will explain a few paragraphs below. The rest of the LHS terms are transport terms for energy, depending on ϕ^* (which induces electron current, and, thus, electron enthalpy transport) and T_e (which induces electron current and heat conduction). In all these terms, potential energy transport is also taken into account. The RHS has two main contributions: the energy variation due to mass varying in time and the energy change associated to ionization. In the RHS the potential energy is also accounted for.

The coefficients in the equation are:

$$\Sigma_j=\left[\frac{T_e}{e}\left(\frac{5}{2}-\ln n_e\right)-\phi^*\right]\sigma_j \tag{1.24}$$

$$\Gamma_j=\left[\frac{T_e}{e}\ln n_e\left(\frac{7}{2}-\ln n_e\right)-\phi^*(\ln n_e-1)\right]\sigma_j \tag{1.25}$$

where $j=H,\perp$.

Equation 1.23 is obtained by using that:

$$-\mathbf{j}_e\cdot\nabla\phi=-\nabla\cdot(\mathbf{j}_e\phi)+\phi\nabla\cdot\mathbf{j}_e \tag{1.26}$$

Taking into account that charge conservation for the electron species is

$$-\frac{\partial}{\partial t}(en_e)+\nabla\cdot\mathbf{j}_e=-en_e\nu_i, \tag{1.27}$$

the final expression for the Joule heating is:

$$-\mathbf{j}_e \cdot \nabla\phi = -\nabla \cdot (\mathbf{j}_e\phi) + \phi\frac{\partial}{\partial t}(en_e) - \phi en_e \nu_i \tag{1.28}$$

1.2.4 Summary

Equations 1.12, 1.13, 1.22 and 1.23 can be solved for ϕ^*, T_e, j_{eb} and q_{eb}.

1.3 Integration along magnetic lines

In this problem, two quantities, ϕ^* and T_e, are constant along the lines. Thus, the problem is, basically, 2D. Considering this, the problem can be solved in some other, more natural, coordinates. Let us define λ_1, λ_2 and s such as:

$$\hat{\mathbf{b}} \cdot \nabla\lambda_1 = 0 \tag{1.29}$$

$$\hat{\mathbf{b}} \cdot \nabla\lambda_2 = 0 \tag{1.30}$$

$$\frac{\partial \mathbf{x}}{\partial s} = \hat{\mathbf{b}} \tag{1.31}$$

where $\mathbf{x} = (x, y, z)$ are the spatial coordinates.

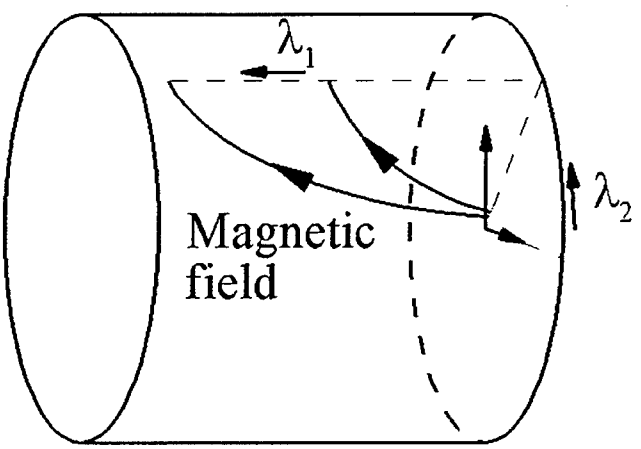

Figure 1.2. Magnetic coordinates λ_1 and λ_2 in an axil-symmetric magnetic field.

Note that λ_1 and λ_2 are two variables that define each magnetic field line (thus, these variables are constant along magnetic field lines).

We require $\nabla s \cdot (\nabla\lambda_1 \times \nabla\lambda_2) = 0$. We can also impose $\nabla\lambda_1 \cdot \nabla\lambda_2 = 0$, but this last condition is very restrictive and can be relaxed.

As an example, consider a magnetic field with cylindrical symmetry. In this case, the variables λ_1 and λ_2 could be the magnetic flux function and the azimuthal angle (see figure 1.2)

In this new reference system, the divergence of a vector $\mathbf{V}$ is:

$$\nabla \cdot \mathbf{V} = \nabla s.\frac{\partial \mathbf{V}}{\partial s} + \nabla \lambda_1.\frac{\partial \mathbf{V}}{\partial \lambda_1} + \nabla \lambda_2.\frac{\partial \mathbf{V}}{\partial \lambda_2} \tag{1.32}$$

In the new reference system, the volume integrals must be done considering:

$$dx\,dy\,dz = ds\,d\lambda_1\,d\lambda_2 \frac{\partial \mathbf{x}}{\partial s}\cdot\left(\frac{\partial \mathbf{x}}{\partial \lambda_1}\times\frac{\partial \mathbf{x}}{\partial \lambda_2}\right) \tag{1.33}$$

Then, the integral of the divergence of $\mathbf{V}$ must be:

$$dx\,dy\,dz\,\nabla\cdot\mathbf{V} = ds\,d\lambda_1\,d\lambda_2 \frac{\partial \mathbf{x}}{\partial s}\cdot\left(\frac{\partial \mathbf{x}}{\partial \lambda_1}\times\frac{\partial \mathbf{x}}{\partial \lambda_2}\right)\left[\nabla s.\frac{\partial \mathbf{V}}{\partial s} + \nabla \lambda_1.\frac{\partial \mathbf{V}}{\partial \lambda_1} + \nabla \lambda_2.\frac{\partial \mathbf{V}}{\partial \lambda_2}\right] \tag{1.34}$$

To simplify this expression, first consider the following equivalences:

$$\frac{\partial \mathbf{x}}{\partial s}\cdot\left(\frac{\partial \mathbf{x}}{\partial \lambda_1}\times\frac{\partial \mathbf{x}}{\partial \lambda_2}\right)\nabla s = \frac{\nabla s}{\nabla s\cdot(\nabla\lambda_1\times\nabla\lambda_2)} = \frac{\nabla s}{|\nabla\lambda_1\times\nabla\lambda_2|} = \frac{\partial \mathbf{x}}{\partial \lambda_1}\times\frac{\partial \mathbf{x}}{\partial \lambda_2} \tag{1.35}$$

$$\frac{\partial \mathbf{x}}{\partial s}\cdot\left(\frac{\partial \mathbf{x}}{\partial \lambda_1}\times\frac{\partial \mathbf{x}}{\partial \lambda_2}\right)\nabla \lambda_1 = \frac{\nabla \lambda_1}{\nabla s\cdot(\nabla\lambda_1\times\nabla\lambda_2)} = \frac{\nabla \lambda_1}{|\nabla\lambda_1\times\nabla\lambda_2|} = -\frac{\partial \mathbf{x}}{\partial s}\times\frac{\partial \mathbf{x}}{\partial \lambda_2} \tag{1.36}$$

$$\frac{\partial \mathbf{x}}{\partial s}\cdot\left(\frac{\partial \mathbf{x}}{\partial \lambda_1}\times\frac{\partial \mathbf{x}}{\partial \lambda_2}\right)\nabla \lambda_2 = \frac{\nabla \lambda_2}{\nabla s\cdot(\nabla\lambda_1\times\nabla\lambda_2)} = \frac{\nabla \lambda_2}{|\nabla\lambda_1\times\nabla\lambda_2|} = \frac{\partial \mathbf{x}}{\partial s}\times\frac{\partial \mathbf{x}}{\partial \lambda_1} \tag{1.37}$$

In these equations we have used $\nabla\lambda_1\times\nabla\lambda_2 = \hat{\mathbf{b}}\,|\nabla\lambda_1\times\nabla\lambda_2|$ and $\hat{\mathbf{b}}\cdot\nabla s = {}^{\partial \mathbf{x}}\!/_{\partial s}\cdot\nabla s = 1$. This does not mean that ∇s is parallel to $\hat{\mathbf{b}}$.

Using equations 1.35, 1.36 and 1.37 to simplify 1.34:

$$dx\,dy\,dz\nabla\cdot\mathbf{V} = ds\,d\lambda_1\,d\lambda_2\left[\frac{\partial}{\partial s}\left(\frac{\nabla s\cdot\mathbf{V}}{|\nabla\lambda_1\times\nabla\lambda_2|}\right) + \frac{\partial}{\partial \lambda_1}\left(\frac{\nabla\lambda_1\cdot\mathbf{V}}{|\nabla\lambda_1\times\nabla\lambda_2|}\right) + \frac{\partial}{\partial \lambda_2}\left(\frac{\nabla\lambda_2\cdot\mathbf{V}}{|\nabla\lambda_1\times\nabla\lambda_2|}\right)\right] \tag{1.38}$$

To get to this equation we have used:

$$\frac{\partial}{\partial s}\left(\frac{\nabla s}{|\nabla\lambda_1\times\nabla\lambda_2|}\right)+\frac{\partial}{\partial\lambda_1}\left(\frac{\nabla\lambda_1}{|\nabla\lambda_1\times\nabla\lambda_2|}\right)+\frac{\partial}{\partial\lambda_2}\left(\frac{\nabla\lambda_2}{|\nabla\lambda_1\times\nabla\lambda_2|}\right)=$$
$$=\frac{\partial}{\partial s}\left(\frac{\partial\mathbf{x}}{\partial\lambda_1}\times\frac{\partial\mathbf{x}}{\partial\lambda_2}\right)-\frac{\partial}{\partial\lambda_1}\left(\frac{\partial\mathbf{x}}{\partial s}\times\frac{\partial\mathbf{x}}{\partial\lambda_2}\right)+\frac{\partial}{\partial\lambda_2}\left(\frac{\partial\mathbf{x}}{\partial s}\times\frac{\partial\mathbf{x}}{\partial\lambda_1}\right)=0 \tag{1.39}$$

Equation 1.38 is important because allows us to simplify the equations. Integrating in s, that is, along magnetic field lines:

$$\int_{s_0}^{s_1}ds\left[\frac{\partial}{\partial s}\left(\frac{\nabla s\cdot\mathbf{V}}{|\nabla\lambda_1\times\nabla\lambda_2|}\right)+\frac{\partial}{\partial\lambda_1}\left(\frac{\nabla\lambda_1\cdot\mathbf{V}}{|\nabla\lambda_1\times\nabla\lambda_2|}\right)+\frac{\partial}{\partial\lambda_2}\left(\frac{\nabla\lambda_2\cdot\mathbf{V}}{|\nabla\lambda_1\times\nabla\lambda_2|}\right)\right]=$$
$$=\left[\frac{\nabla s\cdot\mathbf{V}}{|\nabla\lambda_1\times\nabla\lambda_2|}-\frac{\partial s_B}{\partial\lambda_1}\frac{\nabla\lambda_1\cdot\mathbf{V}}{|\nabla\lambda_1\times\nabla\lambda_2|}-\frac{\partial s_B}{\partial\lambda_2}\frac{\nabla\lambda_2\cdot\mathbf{V}}{|\nabla\lambda_1\times\nabla\lambda_2|}\right]_{s_0}^{s_1}+ \tag{1.40}$$
$$+\frac{\partial}{\partial\lambda_1}\left(\int_{s_0}^{s_1}ds\frac{\nabla\lambda_1\cdot\mathbf{V}}{|\nabla\lambda_1\times\nabla\lambda_2|}\right)+\frac{\partial}{\partial\lambda_2}\left(\int_{s_0}^{s_1}ds\frac{\nabla\lambda_2\cdot\mathbf{V}}{|\nabla\lambda_1\times\nabla\lambda_2|}\right)$$

Here, $s_B(\lambda_1,\lambda_2)$ is the equation that describes the boundaries of our domain. s_B can be s_0 or s_1.

Considering that $F\equiv s-s_B(\lambda_1,\lambda_2)=0$ is the equation for the boundary:

$$\nabla F\equiv\nabla s-\frac{\partial s_B}{\partial\lambda_1}\nabla\lambda_1-\frac{\partial s_B}{\partial\lambda_2}\nabla\lambda_2=k\hat{\mathbf{N}} \tag{1.41}$$

where $\hat{\mathbf{N}}$ is the normal to the boundary, and k is simply the magnitude of the vector. It is also true that:

$$k\hat{\mathbf{b}}\cdot\hat{\mathbf{N}}=\hat{\mathbf{b}}\cdot\nabla s-\frac{\partial s_B}{\partial\lambda_1}\hat{\mathbf{b}}\cdot\nabla\lambda_1-\frac{\partial s_B}{\partial\lambda_2}\hat{\mathbf{b}}\cdot\nabla\lambda_2=\frac{\partial\mathbf{x}}{\partial s}\cdot\nabla s=1 \tag{1.42}$$

Then, $k=1/(\hat{\mathbf{b}}\cdot\hat{\mathbf{N}})$ and we can write:

$$\nabla s-\frac{\partial s_B}{\partial\lambda_1}\nabla\lambda_1-\frac{\partial s_B}{\partial\lambda_2}\nabla\lambda_2=\frac{\hat{\mathbf{N}}}{\hat{\mathbf{b}}\cdot\hat{\mathbf{N}}} \tag{1.43}$$

Finally, the integral of the divergence of $\mathbf{V}$ along the magnetic field lines can be written as:

$$\int_{\text{along }\hat{\mathbf{b}}} dx\,dy\,dz\,\nabla\cdot\mathbf{V} = d\lambda_1\,d\lambda_2\left[\left.\frac{V_N}{(\hat{\mathbf{b}}\cdot\hat{\mathbf{N}})\,|\nabla\lambda_1\times\nabla\lambda_2\,|}\right|_{s=s_0} + \left.\frac{V_N}{(\hat{\mathbf{b}}\cdot\hat{\mathbf{N}})\,|\nabla\lambda_1\times\nabla\lambda_2\,|}\right|_{s=s_1} + \right.$$
$$\left. + \frac{\partial}{\partial\lambda_1}\left(\int_{s_0}^{s_1} ds\,\frac{\nabla\lambda_1\cdot\mathbf{V}}{|\nabla\lambda_1\times\nabla\lambda_2\,|}\right) + \frac{\partial}{\partial\lambda_2}\left(\int_{s_0}^{s_1} ds\,\frac{\nabla\lambda_2\cdot\mathbf{V}}{|\nabla\lambda_1\times\nabla\lambda_2\,|}\right)\right] \tag{1.44}$$

where $V_N = \mathbf{V}\cdot\hat{\mathbf{N}}$.

Let us apply this to equation 1.13. Among other terms, we will find:

$$\frac{\partial}{\partial\lambda_1}\left(\int_{s_0}^{s_1} ds\,\frac{\sigma_H\nabla\lambda_1\cdot(\hat{\mathbf{b}}\times\nabla\phi^*)}{|\nabla\lambda_1\times\nabla\lambda_2\,|}\right) + \frac{\partial}{\partial\lambda_2}\left(\int_{s_0}^{s_1} ds\,\frac{\sigma_H\nabla\lambda_2\cdot(\hat{\mathbf{b}}\times\nabla\phi^*)}{|\nabla\lambda_1\times\nabla\lambda_2\,|}\right) \tag{1.45}$$

Considering that $\hat{\mathbf{b}}\cdot\nabla\phi^* = 0$:

$$\nabla\phi^* = \nabla\lambda_1\frac{\partial\phi^*}{\partial\lambda_1} + \nabla\lambda_2\frac{\partial\phi^*}{\partial\lambda_2} \tag{1.46}$$

We also know that $\hat{\mathbf{b}}\cdot(\nabla\lambda_1\times\nabla\lambda_2) = |\nabla\lambda_1\times\nabla\lambda_2\,|$. Then:

$$\frac{\partial}{\partial\lambda_1}\left(\int_{s_0}^{s_1} ds\,\frac{\sigma_H\nabla\lambda_1\cdot(\hat{\mathbf{b}}\times\nabla\phi^*)}{|\nabla\lambda_1\times\nabla\lambda_2\,|}\right) + \frac{\partial}{\partial\lambda_2}\left(\int_{s_0}^{s_1} ds\,\frac{\sigma_H\nabla\lambda_2\cdot(\hat{\mathbf{b}}\times\nabla\phi^*)}{|\nabla\lambda_1\times\nabla\lambda_2\,|}\right) =$$
$$= -\frac{\partial}{\partial\lambda_1}\left(\bar{\sigma}_H\frac{\partial\phi^*}{\partial\lambda_2}\right) + \frac{\partial}{\partial\lambda_2}\left(\bar{\sigma}_H\frac{\partial\phi^*}{\partial\lambda_1}\right) = -\frac{\partial\bar{\sigma}_H}{\partial\lambda_1}\frac{\partial\phi^*}{\partial\lambda_2} + \frac{\partial\bar{\sigma}_H}{\partial\lambda_2}\frac{\partial\phi^*}{\partial\lambda_1} \tag{1.47}$$

where

$$\bar{\sigma}_H = \int_{s_0}^{s_1} ds\,\sigma_H \tag{1.48}$$

Another term that will appear is:

$$\frac{\partial}{\partial\lambda_1}\left(\int_{s_0}^{s_1} ds\,\frac{\sigma_H\nabla\lambda_1\cdot\nabla_\perp\phi^*}{|\nabla\lambda_1\times\nabla\lambda_2\,|}\right) + \frac{\partial}{\partial\lambda_2}\left(\int_{s_0}^{s_1} ds\,\frac{\sigma_H\nabla\lambda_2\cdot\nabla_\perp\phi^*}{|\nabla\lambda_1\times\nabla\lambda_2\,|}\right) =$$
$$= \frac{\partial}{\partial\lambda_1}\left(\bar{\sigma}_{\perp,11}\frac{\partial\phi^*}{\partial\lambda_1}\right) + \frac{\partial}{\partial\lambda_1}\left(\bar{\sigma}_{\perp,12}\frac{\partial\phi^*}{\partial\lambda_2}\right) + \frac{\partial}{\partial\lambda_2}\left(\bar{\sigma}_{\perp,12}\frac{\partial\phi^*}{\partial\lambda_1}\right) + \frac{\partial}{\partial\lambda_2}\left(\bar{\sigma}_{\perp,22}\frac{\partial\phi^*}{\partial\lambda_2}\right) \tag{1.49}$$

where

$$\bar{\sigma}_{\perp,ij} = \int_{s_0}^{s_1} ds\,\sigma_\perp\frac{\nabla\lambda_i\cdot\nabla\lambda_j}{|\nabla\lambda_1\times\nabla\lambda_2\,|} \quad \text{for } i=1,2,\ j=1,2 \tag{1.50}$$

In a case where $\nabla\lambda_1 \cdot \nabla\lambda_2 = 0$, the equations are simpler because $\bar{\sigma}_{\perp,12} = \bar{\sigma}_{\perp,21} = 0$, $\bar{\sigma}_{\perp,11} = \int ds \sigma_\perp |\nabla\lambda_1| / |\nabla\lambda_2|$ and $\bar{\sigma}_{\perp,22} = \int ds \sigma_\perp |\nabla\lambda_2| / |\nabla\lambda_1|$.

Working all terms similarly, equation 1.13 becomes:

$$
\begin{aligned}
&-\frac{\partial\bar{\sigma}_H}{\partial\lambda_1}\frac{\partial\phi^*}{\partial\lambda_2}+\frac{\partial\bar{\sigma}_H}{\partial\lambda_2}\frac{\partial\phi^*}{\partial\lambda_1}+\frac{\partial\bar{\gamma}_H}{\partial\lambda_1}\frac{\partial}{\partial\lambda_2}\frac{T_e}{e}-\frac{\partial\bar{\gamma}_H}{\partial\lambda_2}\frac{\partial}{\partial\lambda_1}\frac{T_e}{e}+\\
&+\frac{\partial}{\partial\lambda_1}\left(\bar{\sigma}_{\perp,11}\frac{\partial\phi^*}{\partial\lambda_1}+\bar{\sigma}_{\perp,12}\frac{\partial\phi^*}{\partial\lambda_2}\right)+\frac{\partial}{\partial\lambda_2}\left(\bar{\sigma}_{\perp,12}\frac{\partial\phi^*}{\partial\lambda_1}+\bar{\sigma}_{\perp,22}\frac{\partial\phi^*}{\partial\lambda_2}\right)-\\
&-\frac{\partial}{\partial\lambda_1}\left(\bar{\gamma}_{\perp,11}\frac{\partial}{\partial\lambda_1}\frac{T_e}{e}+\bar{\gamma}_{\perp,12}\frac{\partial}{\partial\lambda_2}\frac{T_e}{e}\right)-\frac{\partial}{\partial\lambda_2}\left(\bar{\gamma}_{\perp,12}\frac{\partial}{\partial\lambda_1}\frac{T_e}{e}+\bar{\gamma}_{\perp,22}\frac{\partial}{\partial\lambda_2}\frac{T_e}{e}\right)= \qquad (1.51)\\
&=\frac{\partial}{\partial\lambda_1}\left(\int_{s_0}^{s_1} ds\frac{\nabla\lambda_1\cdot\mathbf{j}_i}{|\nabla\lambda_1\times\nabla\lambda_2|}\right)+\frac{\partial}{\partial\lambda_2}\left(\int_{s_0}^{s_1} ds\frac{\nabla\lambda_2\cdot\mathbf{j}_i}{|\nabla\lambda_1\times\nabla\lambda_2|}\right)+\\
&+\frac{j_{iN}+j_{eN}}{(\hat{\mathbf{b}}\cdot\hat{\mathbf{N}})|\nabla\lambda_1\times\nabla\lambda_2|}\Bigg|_{s=s_0}+\frac{j_{iN}+j_{eN}}{(\hat{\mathbf{b}}\cdot\hat{\mathbf{N}})|\nabla\lambda_1\times\nabla\lambda_2|}\Bigg|_{s=s_1}
\end{aligned}
$$

Similarly, equation 1.23 becomes:

$$
\begin{aligned}
&\left[\int_{s_0}^{s_1}\frac{3}{2}\frac{en_e}{|\nabla\lambda_1\times\nabla\lambda_2|}ds\right]\frac{\partial}{\partial t}\frac{T_e}{e}+\\
&+\frac{Q_{eN}}{(\hat{\mathbf{b}}\cdot\hat{\mathbf{N}})|\nabla\lambda_1\times\nabla\lambda_2|}\Bigg|_{s=s_0}+\frac{Q_{eN}}{(\hat{\mathbf{b}}\cdot\hat{\mathbf{N}})|\nabla\lambda_1\times\nabla\lambda_2|}\Bigg|_{s=s_1}\\
&-\frac{\partial\bar{\Sigma}_H}{\partial\lambda_1}\frac{\partial\phi^*}{\partial\lambda_2}+\frac{\partial\bar{\Sigma}_H}{\partial\lambda_2}\frac{\partial\phi^*}{\partial\lambda_1}+\frac{\partial\bar{\Gamma}_H}{\partial\lambda_1}\frac{\partial}{\partial\lambda_2}\frac{T_e}{e}-\frac{\partial\bar{\Gamma}_H}{\partial\lambda_2}\frac{\partial}{\partial\lambda_1}\frac{T_e}{e}+\\
&+\frac{\partial}{\partial\lambda_1}\left(\bar{\Sigma}_{\perp,11}\frac{\partial\phi^*}{\partial\lambda_1}+\bar{\Sigma}_{\perp,12}\frac{\partial\phi^*}{\partial\lambda_2}\right)+\frac{\partial}{\partial\lambda_2}\left(\bar{\Sigma}_{\perp,12}\frac{\partial\phi^*}{\partial\lambda_1}+\bar{\Sigma}_{\perp,22}\frac{\partial\phi^*}{\partial\lambda_2}\right)- \qquad (1.52)\\
&-\frac{\partial}{\partial\lambda_1}\left(\bar{\Gamma}_{\perp,11}\frac{\partial}{\partial\lambda_1}\frac{T_e}{e}+\bar{\Gamma}_{\perp,12}\frac{\partial}{\partial\lambda_2}\frac{T_e}{e}\right)-\frac{\partial}{\partial\lambda_2}\left(\bar{\Gamma}_{\perp,12}\frac{\partial}{\partial\lambda_1}\frac{T_e}{e}+\bar{\Gamma}_{\perp,22}\frac{\partial}{\partial\lambda_2}\frac{T_e}{e}\right)=\\
&=\int_{s_0}^{s_1}\frac{ds}{|\nabla\lambda_1\times\nabla\lambda_2|}\left[-\left(\frac{3}{2}\frac{T_e}{e}-\phi\right)\frac{\partial}{\partial t}(en_e)+en_e\nu_i\left(-\alpha\frac{E_i}{e}-\phi\right)\right]
\end{aligned}
$$

where Q_{eN} is the total energy flux perpendicular to the boundary

$$
Q_{eN} = q_{eN} - j_{eN}\left(\frac{5}{2}\frac{T_e}{e}-\phi\right) \qquad (1.53)
$$

These equations are equations for ϕ^* and T_e. Before, j_{eb} and q_{eb} were also unknowns, but integrating along the lines has eliminated these variables. This integration has also eliminated the dependence with s. Only the dependence with λ_1 and λ_2 is left. These variables determine univocally each magnetic line. The best way to visualize these variables is considering an axi-symmetric magnetic field. Then, any cylindrical surface is cut once and only once by each magnetic line and each point in the cylindrical surface corresponds univocally to a magnetic line. That is what is plotted in figure 1.2. λ_1 is equivalent to the axial coordinate in the cylinder, and λ_2 is equivalent to the azimuthal angle.

It is interesting to take a look into the form of the equations. There are terms derived from the diamagnetic transport, such that

$$-\frac{\partial \bar{\sigma}_H}{\partial \lambda_1}\frac{\partial \phi^*}{\partial \lambda_2}+\frac{\partial \bar{\sigma}_H}{\partial \lambda_2}\frac{\partial \phi^*}{\partial \lambda_1} \tag{1.54}$$

These terms are characterized by the lack of second derivative and they are usually the higher order terms in the equation (by a factor ω_e / ν_e).

The collisional perpendicular transport terms are diffusion-like, such that

$$\frac{\partial}{\partial \lambda_1}\left(\bar{\sigma}_{\perp,11}\frac{\partial \phi^*}{\partial \lambda_1}+\bar{\sigma}_{\perp,12}\frac{\partial \phi^*}{\partial \lambda_2}\right)+\frac{\partial}{\partial \lambda_2}\left(\bar{\sigma}_{\perp,12}\frac{\partial \phi^*}{\partial \lambda_1}+\bar{\sigma}_{\perp,22}\frac{\partial \phi^*}{\partial \lambda_2}\right) \tag{1.55}$$

Since these equations have been integrated along the magnetic lines, the flows across the boundaries appear, such that

$$\left.\frac{j_{iN}+j_{eN}}{(\hat{\mathbf{b}}\cdot\hat{\mathbf{N}})\,|\nabla\lambda_1\times\nabla\lambda_2|}\right|_{s=s_0}+\left.\frac{j_{iN}+j_{eN}}{(\hat{\mathbf{b}}\cdot\hat{\mathbf{N}})\,|\nabla\lambda_1\times\nabla\lambda_2|}\right|_{s=s_1} \tag{1.56}$$

Any other term is just the corresponding contribution from equations 1.13 and 1.23, integrated along the magnetic field lines.

1.31 Structure of the solution

Both equations 1.51 and 1.52 have similar structure. To study the possible solutions, let us take equation 1.51 in the simplified case $T_e = const.$ and $\nabla\lambda_1.\nabla\lambda_2 = 0$:

$$-\frac{\partial \bar{\sigma}_H}{\partial \lambda_1}\frac{\partial \phi^*}{\partial \lambda_2}+\frac{\partial \bar{\sigma}_H}{\partial \lambda_2}\frac{\partial \phi^*}{\partial \lambda_1}+\frac{\partial}{\partial \lambda_1}\left(\bar{\sigma}_{\perp,11}\frac{\partial \phi^*}{\partial \lambda_1}\right)+\frac{\partial}{\partial \lambda_2}\left(\bar{\sigma}_{\perp,22}\frac{\partial \phi^*}{\partial \lambda_2}\right)=S \tag{1.57}$$

where $\bar{\sigma}_H$, $\bar{\sigma}_{\perp,11}$, $\bar{\sigma}_{\perp,22}$ and S are known functions of λ_1 and λ_2.

Looking at the order of magnitude of the different coefficients, the terms that contain $\bar{\sigma}_H$ are much larger than any other term by a factor ω_e / ν_e. This means that, to zeroth order:

$$-\frac{\partial \bar{\sigma}_H}{\partial \lambda_1}\frac{\partial \phi^*}{\partial \lambda_2}+\frac{\partial \bar{\sigma}_H}{\partial \lambda_2}\frac{\partial \phi^*}{\partial \lambda_1}=0 \tag{1.58}$$

This equation imposes that ϕ^* is constant along the lines $\bar{\sigma}_H = \text{constant}$.

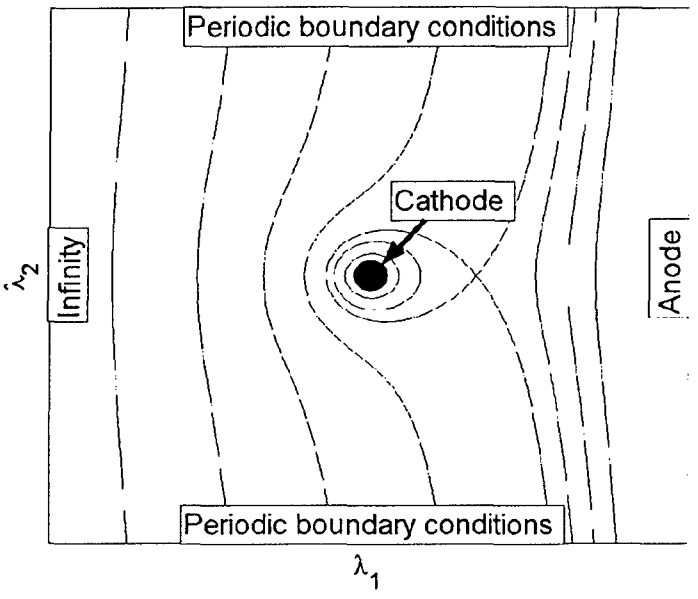

Figure 1.3. Hall thruster representation in a $\lambda_1 - \lambda_2$ plane. $\bar{\sigma}_H$ = const. lines are plotted.

Note that this equation may not (and usually will not) be enough to determine ϕ^*, since its variation across lines of constant $\bar{\sigma}_H$ is left indeterminate by the neglect of the higher order terms. Let us look at an usual Hall thruster configuration plotted in a $\lambda_1 - \lambda_2$ plane (see figure 1.3). Assume that λ_1 and λ_2 are the axial and azimuthal coordinates that locate the magnetic field lines (as seen in figure 1.2). A typical configuration of $\bar{\sigma}_H$ = const. lines is plotted in the λ plane. The boundary conditions are imposed on the upstream and downstream boundaries λ_1 = const. and on the contour of the image of the hollow cathode in the $\lambda_1 - \lambda_2$ plane. In addition, periodicity is imposed on the top and bottom edges. That means that only some of the $\bar{\sigma}_H$ = const. lines have information for ϕ^*. The modified potential in the other lines has to be determined by the next order equation, which contains diffusion terms.

The question about the validity of this approximation naturally arises. We have to pay special attention to the boundaries and the points where the gradient of $\bar{\sigma}_H$ is zero. In the next sections we describe the solutions at those zones.

Solution near the boundaries

At a non-periodic boundary intersected by $\bar{\sigma}_H$ = const. lines, a thin layer may develop. The physical meaning of such a layer will be discussed later. Now, the mathematical solution in such a layer will be studied.

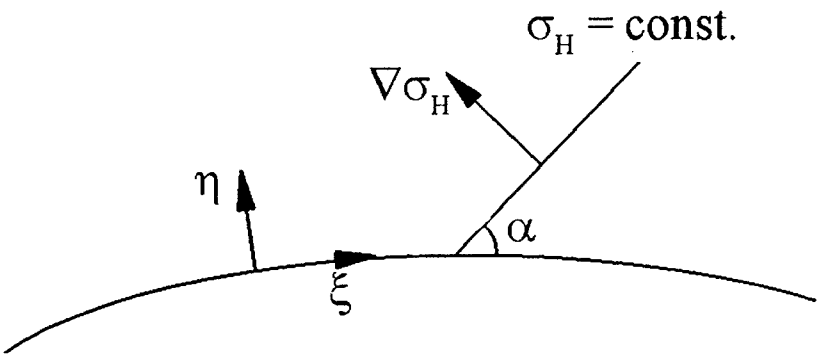

Figure 1.4. Coordinate system tangent to the boundaries. Note that the direction of $\bar{\sigma}_H$ = const. lines is given by angle α.

In the 2D space $\lambda_1 - \lambda_2$ it is possible to define, at least locally, two variables, ξ and η (see figure 1.4), such that the boundary that we are studying is a line η = const. and ξ is perpendicular to η in the sense that

$$\frac{\partial \xi}{\partial \lambda_1}\frac{\partial \eta}{\partial \lambda_1}\bar{\sigma}_{\perp,11} + \frac{\partial \xi}{\partial \lambda_2}\frac{\partial \eta}{\partial \lambda_2}\bar{\sigma}_{\perp,22} = 0 \tag{1.59}$$

In such variables, and considering that the gradients along η are much larger than along ξ, the equation for ϕ^* would be:

$$\bar{\sigma}_{\perp,\eta\eta}\frac{\partial^2 \phi^*}{\partial \eta^2} + \delta\bar{\sigma}_H\left(\sin\alpha\frac{\partial \phi^*}{\partial \eta} + \cos\alpha\frac{\partial \phi^*}{\partial \xi}\right) = 0 \tag{1.60}$$

where

$$\bar{\sigma}_{\perp,\eta\eta} = \left(\frac{\partial \eta}{\partial \lambda_1}\right)^2\bar{\sigma}_{\perp,11} + \left(\frac{\partial \eta}{\partial \lambda_2}\right)^2\bar{\sigma}_{\perp,22} \tag{1.61}$$

$$\delta\bar{\sigma}_H \sin\alpha = -\frac{\partial \bar{\sigma}_H}{\partial \lambda_1}\frac{\partial \eta}{\partial \lambda_2} + \frac{\partial \bar{\sigma}_H}{\partial \lambda_2}\frac{\partial \eta}{\partial \lambda_1} \tag{1.62}$$

$$\delta\bar{\sigma}_H \cos\alpha = -\frac{\partial\bar{\sigma}_H}{\partial\lambda_1}\frac{\partial\xi}{\partial\lambda_2} + \frac{\partial\bar{\sigma}_H}{\partial\lambda_2}\frac{\partial\xi}{\partial\lambda_1} \tag{1.63}$$

$\bar{\sigma}_{\perp,\eta\eta}$, $\delta\bar{\sigma}_H$ and α can be considered functions of ξ only. These parameters do not change appreciably in η – direction compared to what they change in ξ – direction.

Considering that $\bar{\sigma}_{\perp,\eta\eta}/(\xi\,\delta\bar{\sigma}_H) \sim \nu_e/\omega_e << 1$, there are too possible cases:

- $\alpha >> \sqrt{\nu_e/\omega_e}$. In this case, the $\bar{\sigma}_H$ = const. lines are far from being parallel to the boundary. That means that the equation for the solution near the boundary can be written as:

$$\bar{\sigma}_{\perp,\eta\eta}\frac{\partial^2\phi^*}{\partial\eta^2} + \delta\bar{\sigma}_H \sin\alpha\frac{\partial\phi^*}{\partial\eta} = 0 \tag{1.64}$$

  Since $\bar{\sigma}_{\perp,\eta\eta}$, $\delta\bar{\sigma}_H$ and α are only functions of ξ, the general solution to this equation is:

$$\phi^* = A(\xi) + B(\xi)\exp\left(-\frac{\delta\bar{\sigma}_H \sin\alpha}{\bar{\sigma}_{\perp,\eta\eta}}\eta\right) \tag{1.65}$$

  This solution only makes sense when $\sin\alpha > 0$, because otherwise there would be an exponential growth. This means, basically, according to equation 1.62:

$$-\frac{\partial\bar{\sigma}_H}{\partial\lambda_1}\frac{\partial\eta}{\partial\lambda_2} + \frac{\partial\bar{\sigma}_H}{\partial\lambda_2}\frac{\partial\eta}{\partial\lambda_1} > 0 \tag{1.66}$$

  where $\eta(\lambda_1,\lambda_2) = 0$ is the boundary we are interested in, and the vector $(\partial\eta/\partial\lambda_1, \partial\eta/\partial\lambda_2)$ points inwards in the plane $\lambda_1 - \lambda_2$.

  If the condition in equation 1.66 is not satisfied, there is continuity between the boundary condition and the solution because there is no boundary layer solution, that is, the boundary layer solution has exponential growth. This means that the value of ϕ^* in each $\bar{\sigma}_H$ = const. line is given by the boundary conditions on the boundaries that DO NOT SATISFY the condition in equation 1.66. The boundary conditions on the boundaries where equation 1.66 is true do not necessarily determine the thermalized potential in the $\bar{\sigma}_H$ = const. lines: a jump in value occurs across the thin layer.

- $\alpha \sim \sqrt{\nu_e/\omega_e}$. In this case, the $\bar{\sigma}_H$ = const. lines are almost parallel to the boundary. Then, the equation for ϕ^* is equation 1.60.

  This is a parabolic equation, where not only the η dependence is important. No general conclusions can be drawn from this equation. However, the boundaries are not expected in general to be parallel to the $\bar{\sigma}_H$ = const. lines, except in small zones.

The mathematical solution of the problem makes necessary the presence of these boundary layers. The thickness of this layers is $\delta \sim L\,(\nu_e/\omega_e)$ in general, and $\delta \sim L\sqrt{\nu_e/\omega_e}$ when the boundary and the $\bar{\sigma}_H = \text{const.}$ lines are parallel. L is the characteristic length in the problem, associated to the density and magnetic field gradients. The thickness of the layers can be written in terms of the collision mean free path, λ_{mfp}, and the Larmor radius, ρ_L. In such variables, $\delta \sim \rho_L\,(L/\lambda_{\text{mfp}})$. If λ_{mfp} is assumed to be the mean free path of classical electron-neutral collisions, the thickness δ would be a small fraction of the Larmor radius, which makes no physical sense since the Larmor radius is the smallest characteristic length in the problem. To explain this apparent contradiction, we should consider that the electron fluid equations as written are only valid if $\lambda_{\text{mfp}} << L$, or if the classical value of the collision frequency is substituted by a more accurate anomalous transport coefficient. In the case of an anomalous transport collision frequency, the equivalent mean free path is $\lambda_{\text{mfp}} \sim 20\rho_L < L$. Then, the thickness of the layers by the boundaries would be several gyroradii, which is an acceptable value. It seems that these boundary layers, where the collisional perpendicular transport is the most important contribution, must be related to turbulence induced with wavelength of the order of the Larmor radius, since the classical collision mean free path cannot explain their presence. Further study is needed to determine the true nature of these layers.

Solution near extreme points and saddle points of $\bar{\sigma}_H$

At a point where $\partial\bar{\sigma}_H/\partial\lambda_1 = 0$ and $\partial\bar{\sigma}_H/\partial\lambda_2 = 0$, the approximation fails. The gradient of $\bar{\sigma}_H$ can actually be approximated by:

$$\frac{\partial\bar{\sigma}_H}{\partial\lambda_1} \cong \frac{\partial^2\bar{\sigma}_H}{\partial\lambda_1^2}\Delta\lambda_1 + \frac{\partial^2\bar{\sigma}_H}{\partial\lambda_1\partial\lambda_2}\Delta\lambda_2 \tag{1.67}$$

$$\frac{\partial\bar{\sigma}_H}{\partial\lambda_2} \cong \frac{\partial^2\bar{\sigma}_H}{\partial\lambda_1\partial\lambda_2}\Delta\lambda_1 + \frac{\partial^2\bar{\sigma}_H}{\partial\lambda_2^2}\Delta\lambda_2 \tag{1.68}$$

Locally, two new variables, ξ and η, can be defined to simplify the equation. These new variables are defined so that the equation has the following form:

$$\bar{\sigma}_\perp\left(\frac{\partial^2\phi^*}{\partial\xi^2} + \frac{\partial^2\phi^*}{\partial\eta^2}\right) - \xi\frac{\partial^2\bar{\sigma}_H}{\partial\xi^2}\frac{\partial\phi^*}{\partial\eta} + \eta\frac{\partial^2\bar{\sigma}_H}{\partial\eta^2}\frac{\partial\phi^*}{\partial\xi} = 0 \tag{1.69}$$

In this equation, $\bar{\sigma}_\perp$, $\partial^2\bar{\sigma}_H/\partial\xi^2$ and $\partial^2\bar{\sigma}_H/\partial\eta^2$ are almost constant.

The solution of this equation just shows a small zone where the diffusion dominates. This zone is really small and its effect is negligible.

Except for the cases when $\overline{\sigma}_H$ = const. lines intersect non-periodic boundaries, the problem of determining the variation across $\overline{\sigma}_H$ = const. lines is still unsolved. In principle, integration along these "drift lines" will yield one-dimensional differential equations for the variation of the mean variables in the perpendicular ("diffusion") direction. This is now being studied in detail, the difficulty being related to the existence of singular saddle points where these directions are ill-defined. This happens in particular in the vicinity of the cathode's image, because the plasma density, and hence the quantity $\overline{\sigma}_H$, has there a local maximum, immersed in the more general variations due to the main flow. Some other possible techniques are now under consideration, and further results will be available when the M.S. thesis by F. Parra is completed.

2 Application of fluid models to plumes

2.1 Introduction

Work on a fluid model aims to address noise and statistics issues inherent to a discrete approach when simulating a Hall thruster plume expansion. As such, a simplified plasma model has been chosen as an initial test case to confirm that the fluid model works. This preliminary case assumes quasineutrality, no neutrals, no magnetic field, no collisions and neglects electron inertia. Applying these assumptions, the fluid equations are the ambipolar momentum equation, plus the ion conservation equation:

$$\frac{\partial}{\partial t}\left(m_i n_e \mathbf{v}_\mathrm{i}\right) + \nabla \cdot \left(m_i n_e \mathbf{v}_\mathrm{i} \otimes \mathbf{v}_\mathrm{i} + P_e\right) = 0, \tag{2.1}$$

$$\frac{\partial n_e}{\partial t} + \nabla \cdot \left(n_e \mathbf{v}_\mathrm{i}\right) = 0. \tag{2.2}$$

After these are solved, the potential, assuming a polytropic model, follows from,

$$\frac{T_e}{T_{eo}} = \left(\frac{n_e}{n_{eo}}\right)^{\gamma-1}, \tag{2.3}$$

$$\frac{\gamma}{\gamma-1} kT_e - e\phi = \text{constant}. \tag{2.4}$$

Note that Equation 2.3 can be regarded as an interpolating approximation between isentropic flow ($\gamma = 5/3$ for electrons) and isothermal flow ($\gamma = 1$).

Because the form of the fluid plasma equations is hyperbolic, the discontinuous Galerkin method has been chosen as the preferred solution scheme [5]. The power behind discontinuous Galerkin is in the way it merges advantages of both finite volume and finite element methods. The result affords higher-order and thus more accurate solutions at smaller computational cost.

Solving the simplified plasma model axisymmetrically allows verification of our fluid model against existing analytical solutions [6]. In this test case, the expansion of a supersonic jet into vacuum is simulated for comparison to known asymptotic distributions of the plasma properties. Figure 2.1 gives P0 results, constant across elements, for normalized density and Mach number. In these figures, a M~10 jet is issuing from the bottom left corner into vacuum conditions. These low-order results are reasonable -- however, when trying to attain higher-order solutions, numerical difficulties are encountered and no solution is obtained. These problems remain to be resolved and will continue to be worked on.

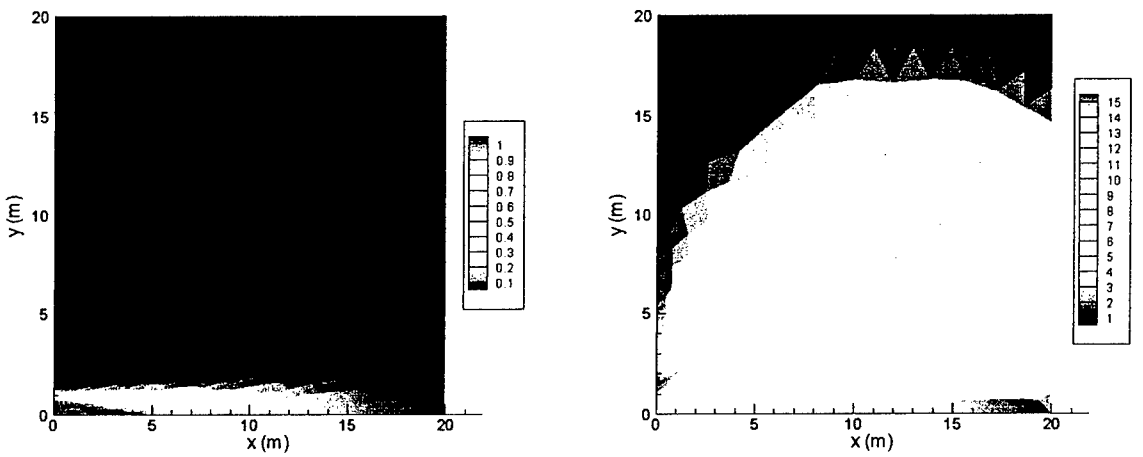

(a) Normalized density (b) Mach number

Figure 2.1. P0 results.

2.2 Far-field model

The purpose of the far-field model is to examine how the bulk plume evolves at greater distances from the thruster exit where the complications of the near-field have already vanished. In this environment, different physics come into play, most notably the effect of the geomagnetic field on the final configuration of the plume. The far-field model aims to expand on previous analytical work and create a numerical model to study this regime.

Formulation of the equations for the far-field model is similar to that for the fluid model, but does not neglect magnetic field. Assumptions made are quasi-neutrality, static

magnetic field and Coulomb-dominated collision interactions. Applying these, the electron momentum equation becomes,

$$\nabla P_e = -en_e(\mathbf{E} + \mathbf{v}_e \times \mathbf{B}) - m_e n_e \nu_e \mathbf{v}_e, \tag{2.5}$$

and assuming the electron gas is perfect, $p_e = n_e kT_e$, the polytropic relationship can be used to express ∇P_e as,

$$\nabla P_e = \frac{\gamma}{\gamma - 1} n_e k \nabla T_e. \tag{2.6}$$

Using the electron current density, $\mathbf{j}_e = -en_e \mathbf{v}_e$ and $\mathbf{E} = -\nabla\phi$, Equation 2.5 can be rearranged to yield,

$$-en_e \nabla\left(\phi - \frac{\gamma}{\gamma - 1}\frac{kT_e}{e}\right) = \mathbf{j}_e \times \mathbf{B} + \frac{m_e \nu_e}{e}\mathbf{j}_e. \tag{2.7}$$

Defining $\phi^* = \phi - \frac{\gamma}{\gamma - 1}\frac{kT_e}{e}$ and $\mathbf{E}^* = -\nabla\phi^*$,

$$\sigma \mathbf{E}^* = \mathbf{j}_e \times \beta + \mathbf{j}_e, \tag{2.8}$$

where $\sigma = \frac{e^2 n_e}{m_e \nu_e}$ and $\beta = \frac{eB}{m_e \nu_e}$.

In the far-field, only the geomagnetic field must be accounted for – in general, the field lines are straight and their interaction with the plume will be determined by their orientation with the thrust axis. Assume for now that $\mathbf{B}_{Earth} = B\hat{z}$. Taking components of Equation 2.8,

$$\mathbf{j}_e = \begin{cases} j_{ex} = \dfrac{\sigma}{1+\beta^2}\left(E_x^* - \beta E_y^*\right) \\ j_{ey} = \dfrac{\sigma}{1+\beta^2}\left(\beta E_x^* + E_y^*\right) \\ j_{ez} = \sigma E_z^* \end{cases} \tag{2.9}$$

One can see that anisotropy in transport arises due to the difference in coefficients of terms parallel and perpendicular to the magnetic field. Perpendicular terms have an additional $\frac{1}{1+\beta^2}$ factor. In general $\beta >> 1$, meaning $\frac{1}{1+\beta^2} << 1$ and transport in the perpendicular direction is much slower than that in the parallel direction.

Assuming steady-state, the continuity equation reduces to $\nabla \cdot \mathbf{j}_e = 0$. Plugging the current density components in and making use of $\mathbf{E}^* = -\nabla\phi^*$, a modified Poisson's equation is obtained,

$$\begin{aligned}
&\frac{\partial^2\phi^*}{\partial x^2} + \frac{\partial^2\phi^*}{\partial y^2} + \beta^2\frac{\partial^2\phi^*}{\partial z^2} \\
&+ \frac{\partial \ln\sigma}{\partial x}\left(\frac{\partial\phi^*}{\partial x} - \beta\frac{\partial\phi^*}{\partial y}\right) + \frac{\partial \ln\sigma}{\partial y}\left(\beta\frac{\partial\phi^*}{\partial x} + \frac{\partial\phi^*}{\partial y}\right) \\
&+ \frac{\partial \ln\beta}{\partial x}\left(\beta\frac{\partial\phi^*}{\partial y} - 2\frac{\partial\phi^*}{\partial x}\right) + \frac{\partial \ln\beta}{\partial y}\left(-\beta\frac{\partial\phi^*}{\partial x} - 2\frac{\partial\phi^*}{\partial y}\right) \\
&+ \beta^2\frac{\partial\phi^*}{\partial z}\frac{\partial \ln\sigma}{\partial z} = 0.
\end{aligned} \tag{2.10}$$

The plan is to approach the far-field model with a hybrid approach, treating ions as particles and electrons as a fluid by solving Equation 2.10. The ion particle distribution is used to find the plasma density, n_e. n_e is then input into the electron equation, solution of which provides the electric field that allows integration of the ion equations to provide the ion distribution for the next time step.

The primary difficulty will lie in solving Equation 2.10 due to the large discrepancy in length scale terms caused by the magnetic field. The problem may be made more tractable by eliminating the anisotropy through a transformation that incorporates the β term into the z coordinate, such as $\frac{\partial}{\partial z'} = \overline{\beta}\frac{\partial}{\partial z}$, where $\beta = \overline{\beta} + \beta'$ ($\overline{\beta}$ represents a constant β over the domain and β' represents the perturbation from the constant value). A similar result would be obtained by using a stretched grid with the elongation in the z coordinate. Employing a coordinate transformation or stretched grid alleviates the length scale difference between x, y and z, but does not help with terms involving β and the x or y coordinate. However, upon closer inspection of these terms in Equation 2.10, it can be seen that they involve products of $\nabla \ln(\sigma/\beta)$ and $\nabla\phi^*$. If ϕ^* and σ/β are related to each other, i.e. $\phi^* = F(\sigma/\beta)$, these cross-terms may cancel one another out and not pose any difficulties to the numerics. Such a situation is plausible since both ϕ^* and σ

are inherently related to the plasma density, n_e. The true nature of the equation will be discovered as this portion of the model is developed further.

REFERENCES

[1] Oh, D.Y., *Computational Modeling of Expanding Plasma Plumes in Space using a PIC-DSMC Algorithm*. Doctor of Science Thesis, Massachusetts Institute of Technology, 1997.

[2] Katz, I., *et al.* "A Hall effect thruster plume model including large-angle elastic scattering." In 37th Joint Propulsion Conference, Salt Lake City, Utah, July 2001.

[3] Provost, S., *et al.*, "Overview of Astrium modeling tool for plasma thruster flow field simulation. IEPC-03-134, 28th International Electric Propulsion Conference, Toulouse, March 2003.

[4] Celik, M., Santi, M., Cheng, S., Martinez-Sanchez, M., and Peraire, J. "Hybrid-PIC simulation of a Hall thruster plume on an unstructured grid with DSMC collisions." In International Electric Propulsion Conference, 2003.

[5] Bassi, F., and S. Rebay. "High-Order Accurate Discontinuous Finite Element Solution of the 2D Euler Equations." *Journal of Computational Physics*, 138:251-285, 1997.

[6] Korsun, A. G., and E. Tverdokhlebova, "The Characteristics of the EP Exhaust Plume in Space." AIAA-97-3065, 33rd AIAA/ASME/SAE/ASEE Joint Propulsion Conference and Exhibit, Seattle, WA, July 1997.